

Garment Refitting for Digital Characters

Fernando de Goes
fernando@pixar.com
Pixar Animation Studios

Donald Fong
dfong@pixar.com
Pixar Animation Studios

Meredith O'Malley
momalley@pixar.com
Pixar Animation Studios



Figure 1: We introduce a new tool that refits garments between different character bodies. In this example, the hoodie was refitted from the left-most male adult to all the other models, the jeans were refitted from the first male adult and female adult to the kid and female teen, respectively, and the pants were refitted from the second male adult to the male teen. ©Disney/Pixar.

ABSTRACT

We present a new technique to refit garments between characters of different shapes. Our approach is based on a novel iterative scheme that alternates relaxation and rebinding optimizations. In the relaxation step, we use affine-invariant coordinates in order to adapt the input 3D garment to the shape of a target character while minimizing mesh distortion. In the rebinding step, we reset the spacing between the refitted garment and the character body controlled by user-prescribed tightness values. Our method also supports additional constraints that encode the spatial and structural arrangement of multi-layers, seams, and fold-overs. We employed this refit tool in Pixar’s feature film *Soul* to transfer garment pieces between various digital characters.

ACM Reference Format:

Fernando de Goes, Donald Fong, and Meredith O’Malley. 2020. Garment Refitting for Digital Characters. In *Special Interest Group on Computer Graphics and Interactive Techniques Conference Talks (SIGGRAPH ’20 Talks)*, August 17, 2020. ACM, New York, NY, USA, 2 pages. <https://doi.org/10.1145/3388767.3407348>

1 OUTLINE

This work aims at deforming a garment mesh \mathcal{G} originally fit to a source character body \mathcal{S} so that it conforms to a target character

Permission to make digital or hard copies of part or all of this work for personal or classroom use is granted without fee provided that copies are not made or distributed for profit or commercial advantage and that copies bear this notice and the full citation on the first page. Copyrights for third-party components of this work must be honored. For all other uses, contact the owner/author(s).

SIGGRAPH ’20 Talks, August 17, 2020, Virtual Event, USA

© 2020 Copyright held by the owner/author(s).

ACM ISBN 978-1-4503-7971-7/20/08.

<https://doi.org/10.1145/3388767.3407348>

body \mathcal{T} . We assume that both source and target bodies share the same mesh connectivity. The vertex positions of the input garment shape are denoted by $\{\bar{x}_v\}$, while their respective refitted points are indicated by $\{x_v\}$. Our refitting strategy is composed of a pre-processing stage (§2) that analyzes the layout of the input garment \mathcal{G} and its tightness relative to the source body \mathcal{S} , followed by an iterative optimization (§3) that compromises mesh distortion with the spatial proximity to the target shape \mathcal{T} .

2 PRE-PROCESSING

We start by describing a series of pre-computation steps that analyze the input models in order to produce geometric features required by our refitting algorithm.

Initial Binding. We bind the 3D position \bar{x}_v of every vertex v in the input garment \mathcal{G} to the closest point \mathbf{p}_v in the source character body \mathcal{S} . We then compute the face f_v in \mathcal{S} containing the projected point \mathbf{p}_v and the displacement vector $\mathbf{d}_v = \bar{x}_v - \mathbf{p}_v$. Each garment vertex v is also assigned to a tightness value m_v set to the vertex area in \mathcal{G} multiplied by a user-prescribed weighting function.

Vertex Stencils. For each garment vertex v , we construct a stencil, denoted by the set \mathcal{N}_v , that gathers any other vertex in \mathcal{G} sharing a face with v . These vertex-based stencils are further augmented with two constraint sets that encode the spatial structure of the input garment. In case UV panels are available, we extract vertices forming panel boundaries and append each boundary set to the stencils of its vertices. To handle multi-layered garments and fold-overs, we expand the vertex stencil \mathcal{N}_v with the cluster of garment vertices that projects to the face f_v in \mathcal{S} . We indicate the number of unique vertices in \mathcal{N}_v by n_v .

Mesh Distortion. Since character bodies often present drastically different shapes, we seek for a refitting tool that supports locally non-rigid deformations, while preserving the edge-spans crafted in the original garment. Following [Budninskiy et al. 2017], we quantify the mesh distortion caused by refitting through affine-invariant coordinates. To compute this representation, we first construct the stencil matrix $\bar{\mathbf{E}}_v = [\dots, \bar{\mathbf{x}}_i - \bar{\mathbf{x}}_v, \dots]$ of size $3 \times n_v$ containing the point vectors connecting v to each element i in \mathcal{N}_v . We then compute the (pseudo-)inverse of the 3×3 covariance matrix associated with the stencil matrix, that is, $\mathbf{C}_v = (\bar{\mathbf{E}}_v \bar{\mathbf{E}}_v^t)^{\dagger}$. Finally, we encode the affine-invariant coordinates by assembling the projection matrix $\mathbf{W}_v = \mathbf{I}_v - \bar{\mathbf{E}}_v^t \mathbf{C}_v \bar{\mathbf{E}}_v$, where \mathbf{I}_v indicates an identity matrix of size $n_v \times n_v$. Importantly, we note that $\bar{\mathbf{E}}_v \mathbf{W}_v = 0$ thus confirming that the projection matrix \mathbf{W}_v is invariant to locally affine transformations. We also point out that \mathbf{W}_v is equivalent to the construction proposed by Budninskiy et al. [2017], but our approach requires no singular value decomposition.

Body Frame Field. Lastly, we use the method of [de Goes et al. 2020] to compute a smooth direction field discretized at the vertices of the polygonal mesh \mathcal{T} . These unit tangent vectors combined with vertex normals define a discrete frame field over \mathcal{T} that enables parallel-transport of displacement vectors along the target body.

3 OPTIMIZATION

We now detail our optimization that outputs points for the garment mesh \mathcal{G} refitted to the target character body \mathcal{T} . Our approach is based on an iterative scheme that alternates mesh relaxation and re-binding steps, which terminate when the largest point difference is less than 0.01% of the model bounding box, or a maximum iteration count (set to 25) is reached.

Initial Warp. Since the character bodies \mathcal{S} and \mathcal{T} share the same mesh connectivity, we initialize the garment refit with a candidate position \mathbf{z}_v for each vertex v corresponding to the projected point \mathbf{p}_v from \mathcal{S} reconstructed in \mathcal{T} and displaced by the vector \mathbf{d}_v warped by the smallest rotation matrix that aligns the face f_v from \mathcal{S} to \mathcal{T} . Figure 2 includes an example of the initial warp.

Relaxation. In this step, we optimize the refitted points $\{\mathbf{x}_v\}$ so that they restore the mesh layout from the original garment \mathcal{G} , while drifting the least from the candidate points $\{\mathbf{z}_v\}$. To do so, we compute points $\{\mathbf{x}_v\}$ that minimize a quadratic objective function of the form $\sum_v \|\mathbf{E}_v \mathbf{W}_v\|^2 + \sum_v m_v \|\mathbf{x}_v - \mathbf{z}_v\|^2$, where the first term penalizes non-affine deformations using the affine-invariant matrices $\{\mathbf{W}_v\}$, versus the second term which accounts for the fitting error relative to the candidate points $\{\mathbf{z}_v\}$ weighted by the tightness values $\{m_v\}$. Since this objective function is quadratic and involves only pre-computed coefficients, the relaxed points can be efficiently solved via a linear system with a pre-factored matrix.

Rebinding. After the relaxation step, the spacing between our refitted garment and the target character body may not match the pre-computed displacement vectors. To better approximate the original values, we rebind the relaxed garment to \mathcal{T} by recomputing the closest points $\{\mathbf{p}_v\}$ and the corresponding projected faces $\{f_v\}$. We also use the smooth frame field defined in \mathcal{T} to reorient the displacement vector \mathbf{d}_v for each garment vertex v relative to the new projection face f_v . By combining the projected point \mathbf{p}_v and

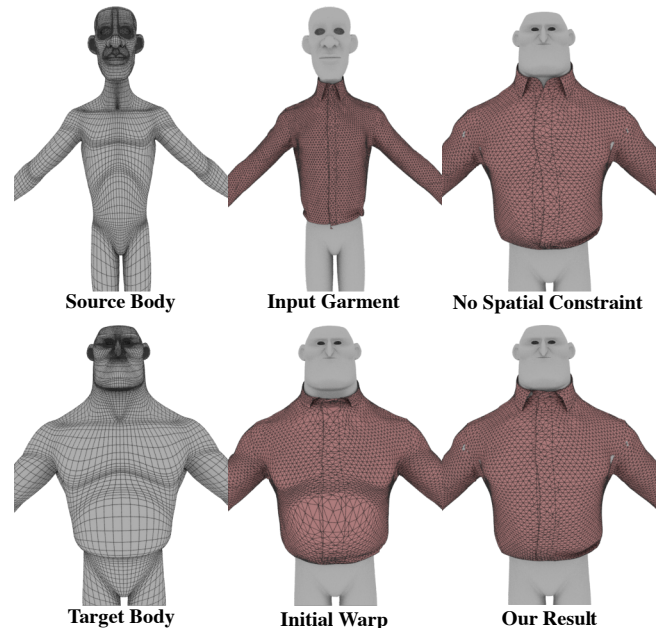


Figure 2: The initial warp rescales the garment from source to target body at the cost of mesh distortion (bottom-center). Our optimization without constraints improves mesh distortion but fails to capture the shirt overlap (top-right). By combining affine-invariant coordinates with spatial constraints, our approach successfully refits the input garment to the target body (bottom-right). ©Disney/Pixar.

the parallel-transported vector \mathbf{d}_v , we obtain an updated candidate point \mathbf{z}_v , which is then fed back to the next relaxation iteration.

Post-Processing. Our optimized garment provides a refit that resembles both the layout and the tightness from the input model. However, our approach does not attempt to remove intersections between the refitted garment and the target body, since some input garments may already be modeled with intersections (see, e.g., the belt area in Figure 2). To resolve any garment-to-body intersection and introduce additional draping details, we run a few iterations of our proprietary cloth simulator as a post-processing step.

4 RESULTS

We implemented our refit tool as a deformer in Maya (see an interactive session in the supplemental video). To optimize the production workflow, we also deployed a script that refits multiple garment poses for various characters all in a single batch. These tools were used in Pixar’s feature film *Soul* enabling garments originally tailored to a specific character to be reused in several models. Figure 1 showcases various garment pieces refitted by our tool between adult and teen models. In Figure 2, we breakdown our method comparing the results with and without spatial constraints versus the initial displacement-based warp.

REFERENCES

- M. Budninskiy, B. Liu, Y. Tong, and M. Desbrun. 2017. Spectral Affine-Kernel Embeddings. *Comput. Graph. Forum (SGP)* 36, 5 (2017), 117–129.
- F. de Goes, A. Butts, and M. Desbrun. 2020. Discrete Differential Operators on Polygonal Meshes. *ACM Trans. Graph.* 39, 4, Article 110 (2020), 14 pages.